# A Solid-State $^{15}N$ CPMAS NMR Study of Dye Tautomerism in Glassy Polystyrene: Site Dependence of Double Minimum Potentials and Their Motional Averaging

**Bernd Wehrle,[1a] Herbert Zimmermann,[1b] and Hans-Heinrich Limbach*,[1a]**

*Contribution from the Institut für Physikalische Chemie der Universität Freiburg i.Br. Albertstrasse 21, D-7800 Freiburg, West Germany, and the Max-Planck Institut für Medizinische Forschung, Jahnstrasse 29, D-6900 Heidelberg, West Germany.*
*Received March 11, 1987*

**Abstract:** We describe matrix effects on the high-resolution solid-state NMR line shapes of bistable molecules that are subject to rapid exchange between two isomers. Matrix effects are modeled in terms of a static superposition of different molecular environments or "sites" characterized by different equilibrium constants, i.e., differently perturbed double minimum potentials of the isomerism. A theory of inhomogeneously broadened NMR line shapes based on this model is presented. In addition, the effects of exchange between the different sites on the NMR line shapes are treated. Site exchange induces homogeneous line broadening and eventually liquid-type NMR spectra, where all molecules experience a similar motionally averaged effective double minimum potential of the isomerism within the NMR time scale. As an example, the variable-temperature $^{15}N$ CPMAS NMR spectra of a $^{15}N$-enriched tetraaza[14]annulene dye (TTAA = 1,8-dihydro-5,7,12,14-tetramethyldibenzo[*b*,*i*]-[$^{15}N_4$]-(1,4,8,11)-tetraazacyclotetradeca-4,6,11,13-tetraene, tetramethyldibenzotetraaza[14]annulene, $C_{22}H_{24}{}^{15}N_4$), in the crystalline state and dissolved in glassy polystyrene, are presented. The $^{15}N$ enrichment of TTAA is described, including the synthesis of its precursor *o*-phenylenediamine-$^{15}N_2$. As reported previously, TTAA is subject to a fast solid-state tautomerism detectable by variable-temperature $^{15}N$ CPMAS NMR spectroscopy. The observation of sharp $^{15}N$ NMR lines for the crystalline compound whose positions are temperature dependent indicates that in the ordered crystal all dye molecules experience the same solid-state perturbation of the tautomeric equilibrium, i.e., all molecules are located in the same site. By contrast, the $^{15}N$ CPMAS spectra of TTAA in glassy disordered polystyrene show a temperature-dependent inhomogeneous line broadening that is detected by two-dimensional NMR experiments. The analysis of the line shapes indicates a broad distribution of different inequivalent TTAA sites with different solid-state perturbations. High-temperature experiments in the region of the glass transition give insight into the way site exchange leads to motionally averaged symmetric double minimum potentials of tautomerism within the NMR time scale. Thus, solid-solution NMR studies provide information about details of molecular rearrangements in a time scale of slow solvent reorientation. In addition, dyes such as tetraaza[14]annulenes can be useful for probing microscopic order and motion in glasses by NMR.

One of the major problems in chemistry is how molecules break and form chemical bonds during a chemical reaction in condensed matter. Little is known about matrix effects on the behavior of reacting molecules in a time scale of slow molecular motion. Information about such effects is necessary for modifying kinetic theories of gas-phase reactions for use in liquids and solids. For example, a reduction of the symmetry of a molecule embedded in condensed phases can influence the reaction mechanism, especially if tunneling is involved, as expected for hydrogen-transfer reactions.[1-3] When studying liquid systems the difficulty arises, however, that molecular environments are not well defined because of the fast molecular motion. Therefore, the study of solid-state reaction systems such as ordered crystals or disordered glasses is especially appealing because the reactants are fixed in time and space. The drawback of such studies is that most reactions require major molecular motions such as translational or rotational diffusion, i.e., processes that are highly restricted in the solid state. Fast chemical solid-state reactions that are decoupled in first order from the motion of the matrix molecules are, therefore, especially important, not only for an understanding of properties of the ordered or disordered solid state[4-6] but also in view of their possible technical application, for example, in the area of future optical information storage devices.[7-11]

It has been shown that variable-temperature (VT) high-resolution solid-state NMR spectroscopy[12-14] of spin $^1/_2$ nuclei such as $^{13}C$, $^{15}N$, etc., under conditions of cross polarization (CP), magic angle spinning (MAS), and $^1H$ decoupling is an excellent tool for establishing fast solid-state reactions.[15-24] Among the fastest reactions studied so far are hydrogen-transfer reactions, where

(1) Bell, R. P. *The Tunnel Effect in Chemistry*; Chapman and Hall: London, 1980.
(2) Brickmann, J.; Zimmermann, H. *Ber. Bunsenges. Phys. Chem.* **1966**, *70*, 157; **1966**, *70*, 521; **1971**, *71*, 160. Brickmann, J.; Zimmermann, H. *J. Chem. Phys.* **1969**, *50*, 1608.
(3) Brickmann, J. *Ber. Bunsenges. Phys. Chem.* **1980**, *84*, 186. Klöffler, M.; Brickmann, J. *Ber. Bunsenges. Phys. Chem.* **1982**, *86*, 203.
(4) Elliott, S. R.; Rao, C. N. R.; Thomas, J. M. *Angew. Chem.* **1986**, *98*, 31; *Angew Chem., Int. Ed. Engl.* **1986**, *25*, 31.
(5) Siebrand, W.; Wildman, T. A. *Acc. Chem. Res.* **1986**, *19*, 238.
(6) Albery, W. J.; Bartlett, P. N.; Wilde, C. P.; Darwent, J. R. *J. Am. Chem. Soc.* **1985**, *107*, 1854.
(7) Friedlich, J.; Haarer, D. *Angew. Chem.* **1984**, *96*, 96; *Angew. Chem., Int. Ed. Engl.* **1984**, *23*, 113.
(8) Völker, S.; van der Waals, J. H. *Mol. Phys.* **1976**, *32*, 1703.
(9) Völker, S.; Macfarlane, R. *IBM Res. Dev.* **1979**, *23*, 547.
(10) Moerner, W. E. *J. Molecular Electronics* **1986**, *1*, 55.
(11) Kämpff, G. *Ber. Bunsenges. Phys. Chem.* **1985**, *89*, 1179.
(12) Schaeffer, J.; Stejskal, E. O. *J. Am. Chem. Soc.* **1976**, *98*, 1031.
(13) Lyerla, J. R.; Yannoni, C. S.; Fyfe, C. A. *Acc. Chem. Res.* **1982**, *15*, 208.
(14) Fyfe, C. A. *Solid State NMR for Chemists*; C. F. C. Press: Guelph, Ontario, 1983.
(15) Szeverenyi, N. M.; Bax, A.; Maciel, G. E. *J. Am. Chem. Soc.* **1983**, *105*, 2579.
(16) Szeverenyi, N. M.; Sullivan, M. J.; Maciel, G. E. *J. Magn. Reson.* **1982**, *47*, 462.
(17) Myrrhe, P. C.; Kruger, J. D.; Hammond, B. L.; Lok, S. M.; Yannoni, C. S.; Macho, V.; Limbach, H. H.; Vieth, H. M. *J. Am. Chem. Soc.* **1984**, *106*, 6079.
(18) Limbach, H. H.; Hennig, J.; Kendrick, R. D.; Yannoni, C. S. *J. Am. Chem. Soc.* **1984**, *106*, 4059.
(19) Limbach, H. H.; Gerritzen, D.; Rumpel, H.; Wehrle, B.; Otting, G.; Zimmermann, H.; Kendrick, R. D.; Yannoni, C. S. In *Photoreaktive Festkörper*; Sixl, H., Friedrich, J., Bräuchle, C., Eds.; Karlsruhe, 1985; p 19-43.
(20) Wehrle, B.; Limbach, H. H.; Köcher, M.; Ermer, O.; Vogel, E. *Angew. Chem.* **1987**, *99*, 914; *Angew. Chem., Int. Ed. Engl.* **1987**, *26*, 934.
(21) Kendrick, R. D.; Friedrich, S.; Wehrle, B.; Limbach, H. H.; Yannoni, C. S. *J. Magn. Reson.* **1985**, *65*, 159.
(22) Limbach, H. H.; Wehrle, B.; Zimmermann, H.; Kendrick, R. D.; Yannoni, C. S. *J. Am. Chem. Soc.* **1987**, *109*, 929.
(23) Limbach, H. H.; Wehrle, B.; Zimmermann, H.; Kendrick, R. D.; Yannoni, C. S. *Angew. Chem.* **1987**, *99*, 241; *Angew. Chem., Int. Ed. Engl.* **1987**, *26*, 247.
(24) Wehrle, B.; Zimmermann, H.; Limbach, H. H. *Ber. Bunsenges. Phys. Chem.* **1987**, *91*, 941.

0002-7863/88/1510-7014$01.50/0 

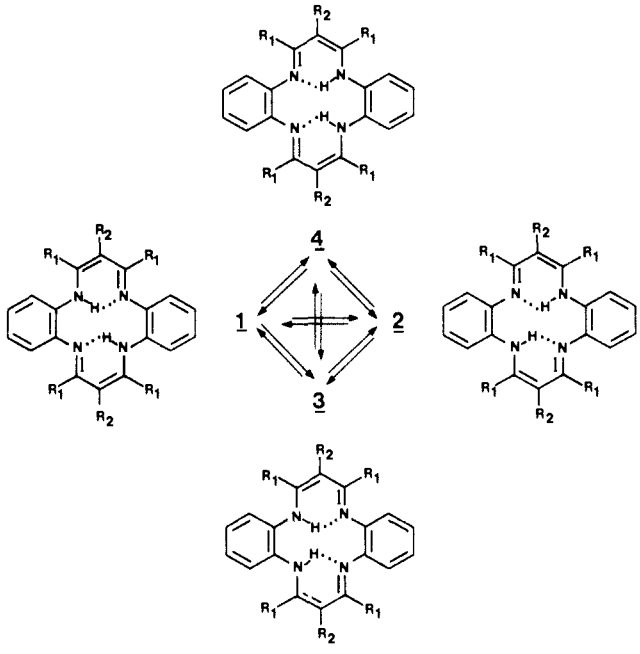

**Figure 1.** The tautomerism of dibenzotetraaza[14]annulenes. DTAA: $R_1 = H$, $R_2 = CH_3$.[32] TTAA: $R_1 = CH_3$ and $R_2 = H$.[33]

protons, hydrogen atoms, or hydride anions migrate between heavy atoms. Several solid-state hydrogen-transfer systems have been studied by natural abundance $^{13}C$ CPMAS NMR.[15-17] However, with the exception of hydride transfers in carbonium ions,[17] carbon atoms are not directly involved in proton transfers and their NMR lines may not always be sensitive to these processes. Therefore, nitrogen NMR is a more suitable method for organic dyes, where nitrogen atoms often act as proton donors or acceptors. Because of the quadrupole moment of the $^{14}N$ nucleus, it is, at present, necessary to enrich the molecules studied with the less abundant spin $^1/_2$ isotope $^{15}N$. Using the $^{15}N$ CPMAS technique of $^{15}N$ enriched compounds we have found, in continuation of previous liquid-state NMR studies,[25-31] fast neutral hydrogen-transfer reactions between nitrogen atoms (tautomerism) in several crystalline dyes such as porphyrines,[18-20] porphycen,[20] phthalocyanine,[19,21] and tetraaza[14]annulenes.[19,22-24] The latter, whose tautomerism is shown in Figure 1, are derivatives of malonaldehyde, i.e., they belong to the class of six-membered H chelates for which it has previously been very difficult to establish the double minimum character of the proton potential.[34-37] The mechanism of the porphin tautomerism is also of theoretical interest.[25,29,38-40] Since the above compounds are dyes they are subject to phototautomerism, even at cryogenic temperatures. This feature has been established for porphyrines and phthalocyanines embedded in organic glasses using laser techniques.[4-7] The astonishing observation that tautomerism in porphyrins and related macrocycles is not suppressed in the solid state can be attributed to the fact that no ionic species are involved, contrary to usual proton-transfer reactions and to the molecular structure, which does not allow the breaking of the intramolecular proton-transfer network by intermolecular hydrogen bond formation. However, this does not mean the absence of solid-state effects on the tautomerism in these compounds. Indeed, one of the results of our previous $^{15}N$ CPMAS NMR studies of these systems is that the gas-phase degeneracy of the tautomers formed by the above dyes is more or less lifted in the crystalline state by intermolecular interactions.[18-24] Because of the periodicity of crystals, all reacting molecules of a sample experience the same solid-state perturbation.

Here we study the question of how the double minimum potential of proton transfer is influenced when the environment is changed from the ordered crystalline to the disordered glassy and, finally, the liquid state. After an experimental section we present theoretical calculations of high-resolution solid-state NMR line shapes of bistable molecules in different types of solid environments. Then we report the results of $^{15}N$ CPMAS NMR experiments performed on the $^{15}N$-enriched tetraaza[14]annulene dye, TTAA[33] (Figure 1), in the crystalline state and dissolved in a solid polystyrene glass. Using the $^{15}N$ nucleus as a spin probe we circumvent the problem of strong $^{13}C$ matrix signals that has so far hindered the observation of dyes in polymers by $^{13}C$ CPMAS NMR. Preliminary results of this system have been presented previously.[22,24] In contrast to the crystalline state, where all dye molecules experience the same solid-state perturbation of the tautomeric equilibrium, we find that TTAA molecules dissolved in glassy polystyrene exist in a multitude of different inequivalent sites with different solid-state equilibrium constants of dye tautomerism. Such glass effects on equilibrium constants of fast reversible reactions have not yet, to our knowledge, been observed. Measurements at higher temperatures show how exchange between the different sites leads to motionally averaged double minimum potentials of tautomerism within the NMR time scale. Finally, the results are discussed.

## Experimental Section

**Synthesis of $^{15}N$-Enriched Compounds.** For the synthesis of $^{15}N$-enriched TTAA we needed *o*-phenylenediamine-$^{15}N_2$ (OPDA) as starting material. Since this compound has not yet, to our knowledge, been prepared, we give a detailed description of its synthesis in the following.

**Synthesis of $^{15}N$-Labeled *o*-Phenylenediamine (OPDA).** The classical synthesis of OPDA via two successive nitrations of benzene with following reductions is inefficient for the synthesis of the $^{15}N$-labeled material in view of the fact that four synthetic steps are required and that OPDA is formed together with *p*-phenylenediamine (PPDA) in approximately equal concentrations. Thus, both compounds have to be separated and half of the $^{15}N$ is lost. Therefore, OPDA was synthesized in one step by reaction of *o*-dichlorobenzene with $^{15}N$-labeled aqueous ammonia in the presence of a catalyst by modifying a procedure proposed by Azuma et al.[41] The aqueous ammonia solution (24.5% p.w.) was prepared as follows. Gaseous ammonia was developed from 95% $^{15}N$-labeled $NH_4Cl$ (A.H. GmbH, Düsseldorf) according to Clusius et al.[42] and condensed into a glass vessel on weighted amounts of ice kept at 195 K. The vessel was then closed and slowly warmed to room temperature. Next 4.8 g of *o*-dichlorobenzene, 1.4 g of Cu powder, 0.2 g of CuCl, and 26.5 g of the aqueous ammonia solution were then heated in an autoclave to 190 °C under continuous stirring. After 3 h a pressure of ca. 30 bar developed, which decreased to about 24 bar after 48 h. After being cooled to room temperature the aqueous solution was extracted 5 times with 100-mL portions of ether. After evaporation of the extract, a crystalline dark brown raw product was obtained which was purified twice by ball tube distillation (1.8 g of a red-brown melt, fp 140–150 °C). The residual

(25) Limbach, H. H.; Hennig, J.; Gerritzen, D.; Rumpel, H. *Faraday Discuss. Chem.* **1982**, *74*, 822.
(26) Gerritzen, D.; Limbach, H. H. *Ber. Bunsenges. Phys. Chem.* **1981**, *85*, 527.
(27) Hennig, J.; Limbach, H. H. *J. Am. Chem. Soc.* **1984**, *106*, 292.
(28) Gerritzen, D.; Limbach, H. H. *J. Am. Chem. Soc.* **1984**, *106*, 869.
(29) Limbach, H. H.; Hennig, J.; Stulz, J. *J. Chem. Phys.* **1983**, *78*, 5432. Limbach, H. H. *J. Chem. Phys.* **1984**, *80*, 5343.
(30) Schlabach, M.; Wehrle, B.; Limbach, H. H.; Bunnenberg, E.; Knierzinger, A.; Shu, A. Y. L.; Tolf, B. R.; Djerassi, C. *J. Am. Chem. Soc.* **1986**, *108*, 3856.
(31) Otting, G.; Rumpel, H.; Meschede, L.; Scherer, G.; Limbach, H. H. *Ber. Bunsenges. Phys. Chem.* **1986**, *90*, 1122.
(32) DTAA ≡ 1,8-dihydro-6,13-dimethyldibenzo[*b*,*i*]-[$^{15}N_4$]-(1,4,8,11)-tetraazacyclotetradeca-4,6,11,13-tetraene (dimethyldibenzotetraaza[14]-annulene).
(33) TTAA ≡ 1,8-dihydro-5,7,12,14-tetramethyldibenzo[*b*,*i*]-[$^{15}N_4$]-(1,4,8,11)-tetraazacyclotetradeca-4,6,11,13-tetraene (tetramethyldibenzotetraaza[14]annulene).
(34) Bock, B.; Flatau, K.; Junge, H.; Kuhr, M.; Musso, H. *Angew. Chem.* **1971**, *83*, 239; *Angew. Chem., Int. Ed. Engl.* **1971**, *83*, 2251.
(35) Limbach, H. H.; Seiffert, W. *Ber. Bunsenges. Phys. Chem.* **1974**, *78*, 532; **1974**, *78*, 641.
(36) Baugham, S. L.; Duerst, R. W.; Rowe, W. F.; Smith, Z.; Wilson, E. B. *J. Am. Chem. Soc.* **1981**, *103*, 6296.
(37) Goedken, V. L.; Pluth, J. J.; Peng, S. M.; Bursten, B. *J. Am. Chem. Soc.* **1976**, *98*, 8014.
(38) Sarai, A. *J. Chem. Phys.* **1982**, *76*, 5554; **1984**, *80*, 5431.
(39) Bersuker, G. I.; Polinger, V. Z. *Chem. Phys.* **1984**, *86*, 57.
(40) Siebrand, W.; Wildman, T. A.; Zgierski, M. Z. *J. Am. Chem. Soc.* **1984**, *106*, 57; **1984**, *106*, 4089.
(41) Azuma, H.; Ohta, J.; Watanabe, H., Patent Agency Japan Patent 51-59824, 1974.
(42) Clusius, K.; Effenberger, E. *Helv. Chim. Acta* **1955**, *38*, 1836.

aqueous phase was acidified with 20% aqueous HCl, treated with charcoal, filtered, and evaporated. Thus, 13.3 g of solid $^{15}NH_4Cl$ was obtained, which contained a small impurity of copper salts and which could be reused in the above process. As a consequence, the overall loss of $^{15}N$ did not exceed 26%.

**Synthesis of 5,7,12,14-Tetramethyldibenzo[*b*,*i*]-[$^{15}N_4$]-(1,4,8,11)-tetraazacyclotetradeca-4,6,11,13-tetraene-Nickel(II) (Ni-TTAA).** This compound was prepared by a slight modification to the procedure given by L'Eplattenier et al.[43] To 15 mL of $CH_3OH$ (free from acetone), flushed for 10 min with gaseous nitrogen, were added successively 1.15 g of nickel acetate tetrahydrate, 1 g of solid OPDA, and 1.1 g of acetylacetone. The mixture was stirred and refluxed under nitrogen for 48 h, during which time different color changes and a precipitate appeared. The mixture was then kept at −30 °C overnight, filtered, and washed with 5 mL of cold methanol, and then with 25 mL of hot water. The Ni-TTAA residue (530 mg) was then dried in an exsiccator and used without further purification. The filtrate was then evaporated and the residue chromatographed over silica with $CH_2Cl_2$ as solvent. Thus, an additional 80 mg of the pure product were obtained and identified by their mass and NMR spectra as Ni-TTAA.

**Synthesis of 1,8-Dihydro-5,7,12,14-tetramethyldibenzo[*b*,*i*]-[$^{15}N_4$]-(1,4,8,11)-tetraazacyclotetradeca-4,6,11,13-tetraene (TTAA, $C_{22}H_{24}{}^{15}N_4$).** This compound was prepared from Ni-TTAA according to the procedure of L'Eplattenier et al.[43] First 530 mg of Ni-TTAA were dissolved in pure alcohol and 600 mg of gaseous HCl were carefully added at room temperature under continuous stirring. The mixture was then stirred for a further 20 h, during which a white precipitate of TTAA hydrochloride appeared, which was filtered and washed with ethanol and dichloromethane. The hydrochloride was then dissolved at room temperature in 25 mL of water and neutralized slowly under continuous stirring with a saturated solution of sodium carbonate in water, during which a yellow precipitate of TTAA appeared. After further stirring 6 h at room temperature the mixture was filtered. The raw TTAA was then dried in vacuo and recrystallized from benzene/petroleum ether (40–60 °C). Yield 210 mg, fp 228–230 °C. Mass spectra: mass 344 for the unlabeled and 348 for the $^{15}N$-labeled TTAA.

**Sample Preparation and Characterization.** TTAA/polystyrene (PS) samples were prepared as follows. TTAA was dissolved with PS (MN = 136 000 g mol$^{-1}$, MW = 276 000 g mol$^{-1}$) in chloroform; the solvent was then removed as far as possible by evacuating the sample at room temperature for 3 days at $10^{-6}$ Torr.

**Differential thermal analysis (DSC)** of PS (sample 1), PS/residual chloroform (sample 2), and PS/TTAA, 6% p.w./residual chloroform (sample 3), was performed on a Perkin Elmer DSC-7 differential scanning calorimeter at heating rates of 30 K/min in order to obtain the glass transition temperatures. The glass transition temperature $T_g$ of sample 1 was 100 °C, the glass transition region extending between 85 and 110 °C. In samples 2 and 3 this region was found between 65 and 105 °C and between 60 and 100 °C, with $T_g$ values of 86 and 82 °C. Thus, the residual solvent and the dye have the effect of additives which lower the glass transition of PS.

**NMR Measurements.** All NMR experiments were performed on a Bruker CXP 100 pulse FT NMR spectrometer working at 90.02 MHz for protons and at 9.12 MHz for $^{15}N$. The spectrometer is equipped with an 2.1 T electromagnet (gap size of 2.2 cm). The CPMAS experiments were performed with use of a Doty MAS probe[44] adapted for a small magnet gap size. For the longtime stability of the magnetic field and low-temperature operation a toluene-$d_8$ $^2H$ lock was used which could be located near the sample. The rotors had an outer diameter of 5 mm and a length of 1 cm and contained about 50 mg of material. Low-temperature operation of the magic angle spinner assembly was achieved with use of cold nitrogen as the driving gas. For this purpose a homebuilt heat exchanger was used, which has been described previously[21] and which avoids liquefication of the nitrogen spinning gas when liquid nitrogen is used as a cooling medium.

## Theoretical Section

**NMR Line Shapes of Bistable Molecules in Ordered and Disordered Solid Environments.** In this section we study the effects of the order and the motion of solid matrices on the high-resolution NMR spectra of bistable molecules. Bistable molecules interconvert between two isomers or molecular states according to

$$1 \rightleftharpoons 2 \qquad (1)$$

We first summarize the theory of exchange broadened NMR line shapes and discuss the calculated spectra of bistable molecules under various conditions important for high-resolution solid-state NMR studies. Matrix effects on the isomerization of bistable molecules are then modeled in terms of a superposition of different environments or "sites" with different equilibrium constants of the isomerism. This model leads to inhomogeneously broadened NMR spectra when the isomerization is fast. Explicit line shape expressions are derived for the case of a bigaussian site distribution function of the free energy of isomerism. Finally, the problem of interconversion of different sites via molecular motions of the matrix molecules is treated. This process induces dynamic NMR line broadening and, eventually, line narrowing, for which appropriate line shape equations are derived.

**General NMR Line Shape Theory.** The theory of exchange broadened pulse FT NMR spectra has been described previously.[45-49] The free induction decay signal measured in the NMR experiment depends on the off-diagonal elements of the density matrix $\rho$ of the spin ensemble studied. In Liouville space the time dependence of these elements is governed by the master equation

$$d\rho/dt = \mathcal{M}\rho, \ \mathcal{M} = -2\pi i(\mathcal{L} - \nu\epsilon) + \mathcal{R} + \Xi \qquad (2)$$

In eq 2 $\epsilon$ is the unit matrix, $i = \sqrt{-1}$, $\nu$ the frequency in Hz, $\mathcal{L}$ the Liouville operator, $\mathcal{R}$ the transverse part of the Redfield relaxation matrix, and $\Xi$ the operator describing the chemical exchange. Let k and l be indices characterizing the rows and columns of the matrix $\mathcal{M}$. The elements of $\mathcal{M}$ are then written as $\mathcal{M}_{kl}$. k and l correspond to transitions or quantum coherences between the spin states $\alpha$ and $\beta$ respectively to $\alpha'$ and $\beta'$. The elements of $\mathcal{L}$ are given by

$$\mathcal{L}_{kl} = \mathcal{L}_{\alpha\beta\alpha'\beta'} = \mathcal{H}_{\alpha\alpha'}\delta_{\beta\beta'} - \mathcal{H}_{\beta\beta'}\delta_{\alpha\alpha'} \qquad (3)$$

$\delta$ is the Kronecker symbol and $\mathcal{H}$ the hamilton operator that can be written as the sum

$$\mathcal{H} = \sum_{\kappa} \mathcal{H}_{\kappa} \qquad (4)$$

$\mathcal{H}_{\kappa}$ is the hamiltonian of the $\kappa$th environment, isomer, state, etc., which participates in the exchange. $\mathcal{H}_{\kappa}$ acts only on the spin functions in $\kappa$. Thus, each diagonal element of $\mathcal{M}$ can be associated to a certain molecular state $\kappa$. In the absence of spin–spin coupling the Redfield relaxation operator $\mathcal{R}$ is diagonal. Generally, one includes artificial and apparative line broadening in the diagonal elements, given by $-\pi W_0$, where $W_0$ is the effective line width in Hz in the absence of exchange. The exchange operator $\Xi$ depends on the rate constants of the exchange and the particular exchange problem. The dimension of $\mathcal{M}$ is given by the number of NMR transitions. Each transition $n$ is characterized by the position $\Lambda_n^{im}$ and the width $\Lambda_n^{re}$, where $\Lambda_n = \Lambda_n^{re} + i\Lambda_n^{im}$ corresponds to the eigenvalues of the matrix $\mathcal{M}$, calculated by diagonalization of $\mathcal{M}$ according to the transformation

$$\Lambda = C^{-1}\mathcal{M}C \qquad (5)$$

Each transition is also characterized by a complex intensity

$$Q_n = Q_n^{re} + iQ_n^{im} = (\sum_k I_k^- C_{kn}^r)(\sum_l \rho_l(0) C_{nl}^l) \qquad (6)$$

where $I_k^-$ are the elements of the lowering operator, which are unity for one-spin systems, and $\rho_k(0)$ are the elements of the density matrix at $t = 0$ given by

$$\rho_k(0) = f_k x_k I_k^- \qquad (7)$$

Since the elements $I_k^-$ and $\rho_k(0)$ are associated to a given molecular state $\kappa$ the quantities $x_k$ are equal to the mole fractions $x_\kappa$ of this state. $f_k$ describes deviations of the elements $\rho_k(0)$ from $x_k I_k^-$. $f_k$ depends on the pulse sequence used and the type of spin system studied. For simple nonselective 90° pulses applied on one-spin systems all $f_k = 1$. In CPMAS experiments $f_k \neq 1$ because of

(43) L'Eplattenier, F. A.; Pugin, A. *Helv. Chim. Acta* **1975**, *58*, 917.
(44) Ellis, P. D.; Doty, F. D. *Rev. Sci. Instrum.* **1981**, *52*, 1868.
(45) Gutowsky, H. S.; McCall, D. M.; Slichter, C. P. *J. Chem. Phys.* **1953**, *21*, 279.
(46) Kubo, R. *Nuovo Cimento Suppl.* **1957**, *6*, 1063. Sack, R. A. *Mol. Phys.* **1958**, *1*, 163.
(47) Binsch, G. *J. Am. Chem. Soc.* **1969**, *91*, 1304.
(48) Limbach, H. H. *J. Magn. Reson.* **1979**, *36*, 287.
(49) Ernst, R. R.; Bodenhausem, G.; Wokaun, A. *Principles of Nuclear Magnetic Resonance in One and Two Dimensions*; Clarendon Press: Oxford, 1987.

the different polarization dynamics of inequivalent spins. Finally, the line shape function is conveniently written in the form

$$Y(\nu) \sim \sum_n \{[Q_n^{re}\Lambda_n^{re} - Q_n^{re}(\Lambda_n^{im} - 2\pi\nu)]/[(\Lambda_n^{re})^2 + (\Lambda_n^{im} - 2\pi\nu)^2]\} \quad (8)$$

In actual calculations it is only necessary to set up the matrix $\mathcal{M}$ and the vector $\rho(0)$.

**Two-State Exchange.** We consider first the case of a spin $S$ in a bistable molecule that exchanges between two states or isomers **1** and **2** according to eq 1. The equilibrium constant of this reaction is given by

$$K_{12} = x_2/x_1 = k_{12}/k_{21} \quad (9)$$

$x_i$ is the mole fraction of state i and $k_{ij}$ the rate constant for the reaction from i to j. The two-state problem has been treated in terms of modified Bloch theory.[45,46] Considering only isotropic chemical shifts $\nu_{S_i}$ and setting $f_1 = f_2 = 1$, the matrix $\mathcal{M}$ and the vector $\rho(0)$ are given by

$$\mu = \begin{bmatrix} -k_{12} - \pi W_0 + 2\pi i\nu_{S_1} & k_{21} \\ k_{12} & -k_{21} - \pi W_0 + 2\pi i\nu_{S_2} \end{bmatrix}, \quad \rho(0) = \begin{bmatrix} x_1 \\ x_2 \end{bmatrix} \quad (10)$$

because the elements of the vector $\Gamma$ are equal to 1. The NMR line shape of spin $S$ can now easily be calculated by using the equations of the preceding section. Some calculated spectra are shown in Figure 2a, where we take into account the presence of two inequivalent uncoupled spins $S = A$ and $X$ in chemically inequivalent positions. The calculated exchange broadened NMR spectra are then the sum of two independent terms each given by eq 10. We consider in Figure 2a the special case where both spins have equal concentrations and where

$$\nu_{A_1} - \nu_{A_2} = \nu_{X_2} - \nu_{X_1} = \Delta\nu \quad (11)$$

Generally, in the slow exchange regime four lines appear at positions given by the chemical shifts of $A$ and $X$ in the two states, $\nu_{A_1}$, $\nu_{A_2}$, $\nu_{X_1}$, $\nu_{X_2}$. The line intensity ratios $A_2/A_1$ and $X_2/X_1$ correspond to the equilibrium constant $K_{12}$. As $k_{21}$ is increased the lines broaden and coalesce. The positions of the averaged lines $A$ and $X$ are given by

$$\nu_A = x_1\nu_{A_1} + (1 - x_1)\nu_{A_2} = (\nu_{A_1} + K_{12}\nu_{A_2})/(1 + K_{12}) \quad (12)$$

$$\nu_X = x_1\nu_{X_1} + (1 - x_1)\nu_{X_2} = (\nu_{X_1} + K_{12}\nu_{X_2})/(1 + K_{12}) \quad (13)$$

Thus, the equilibrium constant $K_{12}$ can be obtained from the line position in the fast exchange case if the chemical shifts are known.

In most high-resolution solid-state NMR studies the spins $A$ and $X$ correspond to rare isotopes such as $^{13}C$ or $^{15}N$ etc. These nuclei are then either present in natural abundance or the molecules studied are artificially enriched. In the case of doubly labeled molecules or molecules containing the rare spins in natural abundance the signal intensities of $A$ and $X$ are equal as assumed in Figure 2a, by contrast to compounds monolabeled in the $A$ or in the $X$ positions.

**Two-State Exchange in the Presence of Molecular Symmetry.** We consider now the case of bistable molecules where $A$ and $X$ are chemically equivalent in the isolated molecules because of the two-state exchange, but where the equilibrium between the two states **1** and **2** is disturbed in the solid state by intermolecular interactions. As an example consider the case of the proton-transfer systems

$$\underset{\text{state 1}}{^{15}N_AH\cdots{}^{15}N_X} \rightleftarrows \underset{\text{state 2}}{^{15}N_A\cdots H^{15}N_X} \quad (14)$$

$$\underset{\text{state 1}}{^{15}N_AH\cdots{}^{14}N} \rightleftarrows \underset{\text{state 2}}{^{15}N_A\cdots H^{14}N} \quad (15)$$

$$\underset{\text{state 1}}{^{14}NH\cdots{}^{15}N_X} \rightleftarrows \underset{\text{state 2}}{^{14}N\cdots H^{15}N_X} \quad (16)$$

in the solid state. $A$ and $X$ correspond here to $^{15}N$ atoms. Although intermolecular interactions perturb the tautomeric equilibrium, favoring the tautomeric state **1**, they do not lead in good approximation to different chemical shifts of chemically equivalent but crystallographic inequivalent nuclei. This means that for such molecules the relations

$$\nu_{A_1} = \nu_{X_2} \text{ and } \nu_{A_2} = \nu_{X_1} \quad (17)$$

hold in good approximation.

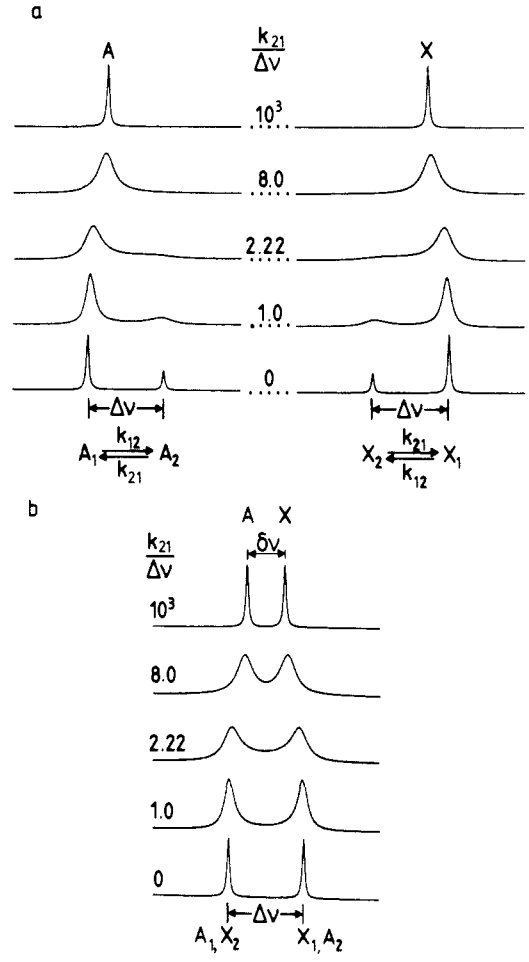


**Figure 2.** Calculated spectra for two single spins $A$ and $X$ located in an asymmetric molecule subject to exchange between two isomers. The equilibrium constant $K_{12} = k_{12}/k_{21}$ of the isomerism was set to a value of 0.33 in all spectra. The values of $k_{21}$ increase from the bottom to the top. For further explanation see text. (a) Spectra caculated for the case that the chemical shifts of all nuclei are different; (b) spectra calculated for the case where $A$ and $X$ are in similar chemical environments, i.e., for the case of the validity of eq 14.

The calculated spectra, assuming the validity of eq 17, are shown in Figure 2b. They are easily obtained by an appropriate superposition of the corresponding subspectra in Figure 2a. In the slow exchange regime, the spectra consist of only two lines of equal intensity which broaden and coalesce into two averaged lines $A$ and $X$ as $k_{21}$ is increased. By combining eq 12, 13, and 17 it follows for the position of these lines in the case of fast exchange that

$$\nu_A = (\nu_{A_1} + K_{12}\nu_{A_2})/(1 + K_{12}) = (\nu_{X_1} + K_{12}^{-1}\nu_{X_2})/(1 + K_{12}^{-1}) \quad (18)$$

and that

$$\nu_X = (\nu_{X_1} + K_{12}\nu_{X_2})/(1 + K_{12}) = (\nu_{A_1} + K_{12}^{-1}\nu_{A_2})/(1 + K_{12}^{-1}) \quad (19)$$

By combination of eq 11, 18, and 19 one obtains for the "reduced splitting"

$$\delta\nu = \nu_X - \nu_A = \Delta\nu\{(1 - K_{12})/(1 + K_{12})\} \quad (20)$$

of lines $A$ and $X$ in the fast exchange regime. From eq 18 and

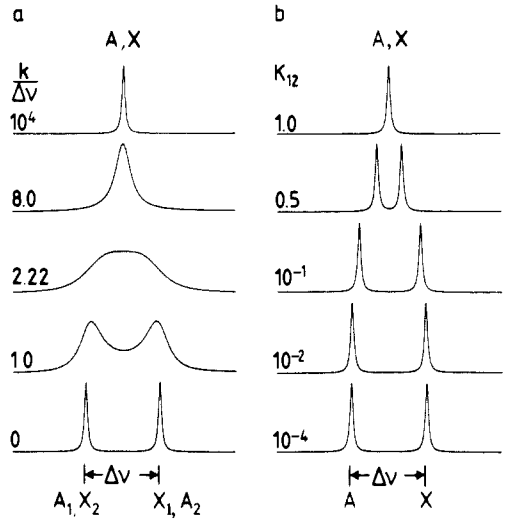


**Figure 3.** (a) Calculated spectra for two single spins $A$ and $X$ located in a symmetric bistable molecule where $K_{12} = 1$. (b) Calculated spectra for two single spins $A$ and $X$ located in an asymmetric bistable molecule in the regime of fast isomerism. $K_{12}$ was varied from 0 to 1.

19 it follows for the case of molecules where eq 17 holds that instead of distinguishing between two types of spins $A$ and $X$ which experience different intrinsic chemical shifts but the same equilibrium constant $K_{12}$ it is equivalent to speak of two isochronous spins which experience the same chemical shift but different equilibrium constants $K_{12}$ and $K_{12}^{-1}$.

The case presented in Figure 2b contains two special subcases that are of practical importance. Figure 3a shows the familiar calculated spectra for a symmetric two-state exchange where $K_{12} = K_{12}^{-1} = k_{12}/k_{21} = 1$. Here, two sharp lines are expected in the slow exchange regime as in Figure 2b, but only one coalesced line in the fast exchange regime above the coalescence point because $\delta\nu = 0$ according to eq 20. In the series of spectra in Figure 3b the exchange between the two states **1** and **2** was assumed to be very fast, but $K_{12}$ was changed from 0 to unity. The line positions were calculated according to eq 20. A comparison of the bottom spectra of Figures 2b, 3a, and 3b shows that the cases of slow exchange with $K_{12} \leq 1$ and the case of fast exchange with $K_{12} \ll 1$ cannot be distinguished. For this purpose, it is necessary to raise the temperature until either line broadening according to Figure 2b or Figure 3a is observed or until the lines move together as shown in Figure 3b. All possibilities expressed in Figures 2b, 3a, and 3b have been observed experimentally for fast proton transfer systems between $^{15}N$ atoms in organic dyes by high-resolution $^{15}N$ CPMAS NMR spectroscopy.[18-24]

**Introduction of Sites with Different Equilibrium Constants of Isomerism.** We consider now the possibility of the presence of different long-lived environments or "sites" where the isomerism of the molecules studied is perturbed in a different way due to intermolecular interactions. We have then to introduce new symbols $m, n = 1, 2, \ldots$ in order to denote the different sites. The actual state of a molecule located in the site $m$, present as isomer $i = 1$ or 2, is then given by $\kappa = im$, $im = 11, 12, \ldots, 21, 22$. If $x_{im}$ is the mole fraction or population of the state $im$, the population of site $m$ is given by $x_m = x_{1m} + x_{2m}$. Thus, let us define a site $m$ as the ensemble of all chemically equivalent nuclei in the sample of interest experiencing the same equilibrium constant

$$K_{1m2m} = x_{2m}/x_{1m} \tag{21}$$

of the isomerism

$$1m \rightleftharpoons 2m \tag{22}$$

with $K_{1m2m} \neq K_{1n2n}$. For example, in the case of the reactions described by eq 14–16 one could speak of two sites $1$ and $2$, characterized by the equilibrium constants $K_{1122}$ and $K_{1222} = K_{1121}^{-1}$, instead of speaking of two different spins $A$ and $X$ characterized by the same equilibrium constant of the two-state exchange. For crystalline environments where the number of sites is small their introduction does, however, not necessarily represent an advantage.

**NMR Spectra of Bistable Molecules Located in a Multitude of Superposed Sites.** The situation is different when bistable molecules embedded in a disordered glass are considered. Here, an infinite number of different sites has to be taken into account. The molecules of a given site will, generally, not be spatially located nearby but will be distributed over the whole sample volume. In other words, here we treat chemically equivalent molecules in different sites as inequivalent "supermolecules" characterized by different equilibrium constants of isomerism; a molecular picture of this model is discussed later in Figure 8.

We consider now the NMR spectra of a bistable molecule embedded in a disordered environment. For this purpose we consider only a finite number $l$ of sites. Furthermore, we restrict our analysis to the case of very fast state exchange between the isomers. Thus, we avoid further distinguishing between "subsites" characterized by the same equilibrium constants but different rate constants of isomerism. It follows then from eq 12 and 13 for the position of the averaged NMR line of spin $S$ in site $m$

$$\nu_m = x_{1m}\nu_{S_{1m}} + (1 - x_{1m})\nu_{S_{2m}} = (\nu_{S_{1m}} + K_{1m2m}\nu_{S_{2m}})/(1 + K_{1m2m}),\ S = A, X, \ldots \tag{23}$$

$\nu_{S_{im}}$ is the chemical shift of spin $S$ in the state $im$. The NMR spectra can now be calculated by associating to each site a lorentzian line of the width $W_0$ and an intensity $P(m)$. There are, however, too many variables in eq 23 in order to make line shape studies based on this equation practicable. First, it is a great simplification if only one type of chemically equivalent nuclei needs to be considered, as is the case in asymmetric molecules containing only one spin label and in symmetric molecules containing several labels for which eq 17 holds. Then, the subscript $S$ can be dropped in eq 23. Furthermore, let us assume that the intrinsic chemical shifts are equal in all sites. Thus,

$$\nu_{S_{1m}} = \nu_{S_{1n}} = \nu_1,\ \nu_{S_{2m}} = \nu_{S_{2n}} = \nu_2 = \nu_1 + \Delta\nu \tag{24}$$

This assumption implies that the signal intensity at a given frequency $\nu$ contains contributions only from one single site $m$ characterized by the average frequency $\nu_m$

$$\nu_m = x_{1m}\nu_1 + (1 - x_{1m})\nu_2 = (\nu_1 + K_{1m2m}\nu_2)/(1 + K_{1m2m}) = \nu_1 + \Delta\nu K_{1m2m}/(1 + K_{1m2m}) \tag{25}$$

Thus, if we consider a total of $l$ sites we can divide the frequency spectrum in $l$ equal portions spaced by $(\nu_2 - \nu_1)/(l - 1)$, which leads to the expression

$$\nu_m = \nu_1 + (m - 1)(\nu_2 - \nu_1)/(l - 1),\ m = 1 \text{ to } l \tag{26}$$

By combining eq 25 and 26 one obtains the equilibrium constant $K_{1m2m}$ which is associated to site $m$, i.e., to the frequency $\nu_m$ as

$$K_{1m2m} = (m - 1)/(l - m) \tag{27}$$

From eq 27 it follows that the site

$$m' = l - m + 1 \tag{28}$$

is characterized by the equilibrium constant

$$K_{1m'2m'} = K_{1m2m}^{-1} \tag{29}$$

Because of eq 29 one may call the sites $m$ and $m'$ "twinned sites" For symmetric molecules for which eq 17 is valid the probabilities

$$P(m) = P(m') \tag{30}$$

of finding both sites are equal, as discussed above.

As an example, in Figure 4 calculated spectra are shown which were generated by taking eq 30 into account. The spectra represent the sum of $l = 11$ lorentzian lines of the width $W_0$, one for each site, with the line position given by eq 25 and intensities calculated as described in the next section. Because of eq 30 the line intensities are symmetric with respect to the line center. In the spectra at the bottom the sites with equilibrium constants $K_{1m2m} \ll 1$ (and the twinned sites with $K_{1m'2m'} \gg 1$) dominate, leading to a characteristic "hole" in the line center. This hole is absent in the spectra at the top where sites with $K_{1m2m} \approx 1$ dominate.

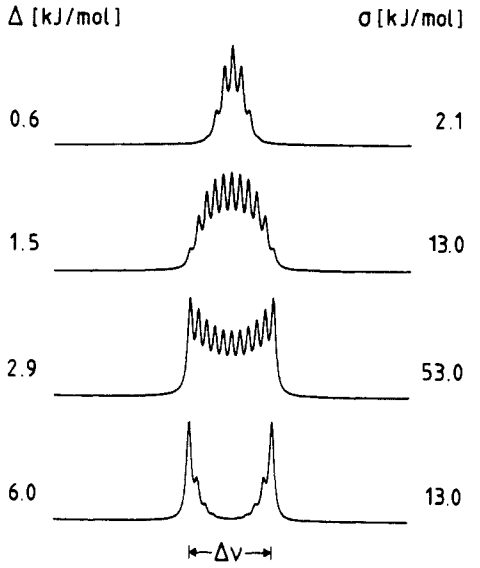


**Figure 4.** Calculated NMR spectra for a static superposition of $l = 11$ sites with different equilibrium constants of fast isomerism. The line positions were calculated with eq 25. The sites were weighed in an arbitrary way according to eq 36, derived in terms of a bigaussian distribution of free reaction enthalpies of the isomerism. Bottom: small equilibrium constants dominate. Top: equilibrium constants close to 1 dominate.

**Site Distribution Function.** In principle, the site distribution function $P(m)$ can be experimentally obtained by total line shape analysis of experimental spectra; in other words, the spectrum *is* the distribution function if $W_0$ were zero. It is, however, convenient in some cases to introduce a continuous distribution function in an analytical form, which is independent of the concept of discrete sites. In the literature, the so-called Williams–Watts distribution[50] has frequently been used to describe rate processes in organic glasses. Also, a gaussian distribution function of free activation energies has been employed.[6] We introduce here a bigaussian distribution function $P(\Delta G_{12})$ of the free reaction enthalpy $\Delta G_{12}$. $\Delta G_{12}$ is related to the equilibrium constants $K_{12}$ by the van't Hoff equation

$$K_{12} = \exp(-\overline{\Delta G_{12}}/RT) \tag{31}$$

$R$ is the gas constant and $T$ the temperature. The function is given by

$$P(\Delta G_{12}) = -\frac{1}{N}\frac{dN}{d\Delta G_{12}} = \frac{1}{2}\sqrt{\frac{\alpha}{\pi}}[\exp\{-\alpha(\Delta G_{12} - \overline{\Delta G_{12}} - \Delta)^2\} + \exp\{-\alpha(\Delta G_{12} - \overline{\Delta G_{12}} + \Delta)^2\}],\ \alpha = 1/(2\sigma^2) \tag{32}$$

$\sigma$ characterizes the width of the two terms, $\overline{\Delta G_{12}} + \Delta$ and $\overline{\Delta G_{12}} - \Delta$ the positions of the two maxima. $\overline{\Delta G_{12}}$ is the mean value of the free energy of isomerism

$$\overline{\Delta G_{12}} = \int_{-\infty}^{+\infty} \Delta G_{12} P(\Delta G_{12})\, d\Delta G_{12} \tag{33}$$

For the mean square value $\overline{\Delta G_{12}^2}$ we obtain

$$\overline{\Delta G_{12}^2} = \int_{-\infty}^{+\infty} P(\Delta G_{12}) \Delta G_{12}^2\, dG_{12} = \overline{\Delta G_{12}^2} + \sigma^2 + \Delta^2 \tag{34}$$

The mean quadratic deviation from the mean value $\overline{\Delta G_{12}}$ is given by

$$\overline{(\Delta G_{12} - \Delta G_{12})^2} = \int_{-\infty}^{+\infty} P(\Delta G_{12})(\Delta G_{12} - \overline{\Delta G_{12}})^2\, dG_{12} = \sigma^2 + \Delta^2 \tag{35}$$

Note that if necessary one could introduce different widths and positions of the maxima for the two terms in eq 32. Using eq 31 it follows that

(50) Williams, G.; Watts, D. C. *Trans. Faraday Soc.* **1970**, *66*, 80.

$$P(K_{12}) = \frac{1}{N}\frac{dN}{dK_{12}} = \frac{1}{N}\frac{dN}{d\Delta G_{12}}\frac{d\Delta G_{12}}{dK_{12}} = -\frac{1}{2}\sqrt{\frac{\alpha}{\pi}}\frac{RT}{K_{12}}[\exp\{-\alpha(-RT\ln K_{12} - \overline{\Delta G_{12}} - \Delta)^2\} + \exp\{-\alpha(-RT\ln K_{12} - \overline{\Delta G_{12}} + \Delta)^2\}] \tag{36}$$

and with eq 12 and 24 that

$$P(\nu) = \frac{1}{N}\frac{dN}{d\nu} = \frac{1}{N}\frac{dN}{dK_{12}}\frac{dK_{12}}{d\nu} = -\sqrt{\frac{\alpha}{\pi}}\frac{RT}{2}\frac{\nu_2 - \nu_1}{(\nu - \nu_2)(\nu_1 - \nu)}\left[\exp\left\{-\alpha\left(RT\ln\frac{\nu_1 - \nu}{\nu - \nu_2} - \overline{\Delta G_{12}} - \Delta\right)^2\right\} + \exp\left\{-\alpha\left(RT\ln\frac{\nu_1 - \nu}{\nu - \nu_2} - \overline{\Delta G_{12}} + \Delta\right)^2\right\}\right] \tag{37}$$

We can now calculate a distribution function for discrete sites by combining eq 26 and 37. We obtain

$$P(m) = \frac{1}{N}\frac{dN}{dm} = \frac{1}{N}\frac{dN}{d\nu}\frac{d\nu}{dm} = \sqrt{\frac{\alpha}{\pi}}\frac{RT}{2}\frac{l-1}{(m-l)(m-1)}\left[\exp\left\{-\alpha\left(RT\ln\frac{m-1}{l-m} - \overline{\Delta G_{12}} + \Delta\right)^2\right\} + \exp\left\{-\alpha\left(RT\ln\frac{m-1}{l-m} - \overline{\Delta G_{12}} - \Delta\right)^2\right\}\right] \tag{38}$$

Equation 38 was used to weigh the sites in Figure 4 and only $\sigma$ and $\Delta$ were varied. In order to ensure the condition expressed by eq 28 we set in Figure 4 the mean free enthalpy

$$\overline{\Delta G_{12}} = -RT\ln\overline{K_{12}} = 0 \tag{39}$$

The temperature was arbitrarily set to 298 K. Since only $l = 11$ sites were considered in Figure 4, the fine structure of the superposed signals is still seen. This fine structure disappears when the number of sites $m$ is increased. The NMR line is then called "inhomogeneously" broadened because the overall line width is constituted by a superposition of individual lines, each having a much smaller "individual" line width. If the latter results from a dynamic linebroadening it is called in optics the "homogeneous" linewidth. Thus, it is not necessary to increase $m$ above a certain point where the separation between the discrete lines becomes smaller than the individual linewidth.

**NMR Line Shapes in the Presence of Site Exchange.** In this section we ask how exchange between the different sites affects the NMR spectra. We will assume that site exchange and isomerism are decoupled from each other in the sense that the rate constants of exchange between two sites $m$ and $n$ are independent of whether the bistable molecule is present as isomer **1** or isomer **2**. The rate constants of interconversion between sites $m$ and $n$ are then denoted by the symbol $k_{mn}$. Since each site contains only one spin characterized by a single averaged Larmor frequency given by eq 25 the elements of the exchange operator are easily written using the principle of detailed balance. One obtains

$$\Xi_{mn} = -\delta_{mn}\sum_{r\neq m} k_{mr} + (1 - \delta_{mn})k_{mn} \tag{40}$$

$\delta_{mn}$ is the Kronecker symbol. The quantity

$$\tau_m^{-1} = \sum_{r\neq m} k_{mr} \tag{41}$$

can be regarded as the average inverse lifetime of site $m$. In eq 40 the different $k_{mn}$ must depend on each other because their number increases with the number of sites and because this number is arbitrary. The true number of parameters describing the exchange is, however, unknown. We, therefore, limit our discussion here to the case where the site exchange can be described by a single correlation time $\tau$. For this purpose we assume that the rate constant $k_{mn}$ is proportional to $\tau^{-1}$, to the mole fraction $x_n$ of site $n$, and to a parameter $D_{mn}$

$$k_{mn} = \tau^{-1}x_n D_{mn} \tag{42}$$

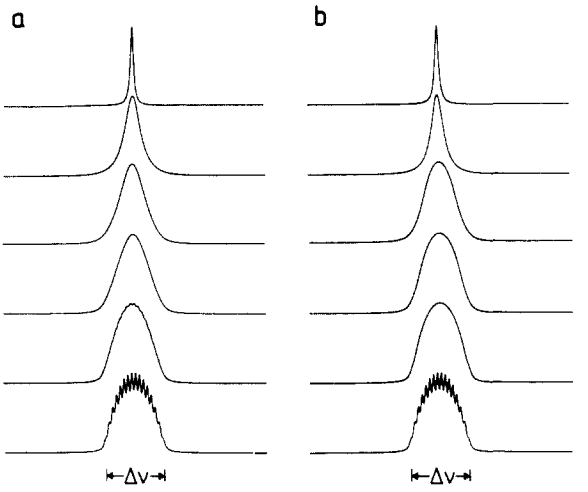


**Figure 5.** Effects of reduced site lifetime $\tau$ on the NMR spectra of spins $A$ and $X$ located in different sites characterized by a bigaussian distribution of free reaction energies of isomerism. The bottom spectra where $\tau = \infty$ was generated in a similar way as the top spectrum in Figure 4, but using $l = 16$ sites. From the bottom to the top only the $\tau$ values were changed. Fast site exchange renders all spins $A$ and $X$ equivalent as follows: (a) ASE model, $\tau^{-1}/\Delta\nu = 0, 0.15, 0.375, 0.75, 1.5, 75$; (b) NSE model, $\tau^{-1}/\Delta\nu = 0, 15, 60, 150, 750, 7500$.

$D_{mn} = D_{nm} = 0$ or 1 depending on whether exchange between sites $m$ and $n$ is allowed or not. The elements of the exchange operator are then given by

$$\Xi_{mn} = -\delta_{mn} \sum_{r \neq m} \tau^{-1} x_r D_{mr} + (1 - \delta_{mn}) \tau^{-1} x_n D_{mn} \qquad (43)$$

One can imagine two working hypotheses that represent two extreme limits of a complex exchange pattern. In limit (i) each site exchanges with every other site, i.e., all $D_{mn} = 1$ (ASE ≡ all site exchange). Since $x_m \ll 1$ because of the great number of sites, it follows from eq 40 that the lifetimes of all sites are equal, i.e., $\tau_m = \tau$. In limit (ii) each site exchanges only with a neighboring site, i.e., the equilibrium constants of state exchange change only gradually in small increments (NSE ≡ neighbor site exchange). In other words, only values of $D_{mn}$ with $m = n \pm 1$ are non-zero. In Figure 5 we compare the calculated NMR line shapes for both limits. In order to demonstrate better the effects of site exchange on the spectra we consider only 16 sites, which leads to 16 separated lines at the bottom of parts a and b of Figure 5, where the average site lifetime $\tau \to \infty$. We use an arbitrary site distribution. As we shorten $\tau$, the homogeneous width of the individual lines first increases, leading to the disappearance of the fine structure, and then all individual lines coalesce into one homogeneously broadened line. In the fast site exchange regime only one sharp line survives. In the coalescence region the ASE model (Figure 5a) shows a "triangular" line shape whereas the NSE line shape still resembles a gaussian line shape. In the slow and the fast exchange regime both models give rise to similar line shapes and can, therefore, not be distinguished by one-dimensional NMR spectroscopy. Note that shorter $\tau$ values are needed in order to obtain coalescence in the NSE model as compared to the ASE model.

**Computer Program.** In order to perform the line shape calculations based on the theory presented in this section a computer program was written in Fortran 77. The program requires the matrix $\mathcal{M}$, the vector $\rho(0)$ defined in eq 2–8, and the quantities $\Delta\nu$, $\sigma$, $\Delta$, $W_0$, $\tau^{-1}$, and $D_{mn}$, defined above, as input. The inhomogeneously broadened spectra in the absence of site exchange shown in Figure 4 were calculated by setting $\tau^{-1} = 0$.

## Results

Using $^{15}N$ CPMAS NMR spectroscopy, we study in this section the question of how the tautomerism of TTAA (Figure 1) is affected by the ordered or disordered solid state. For this purpose experiments were performed on crystalline TTAA and on TTAA dissolved in glassy polystyrene. Preliminary accounts of this work have been reported previously.[22,24]

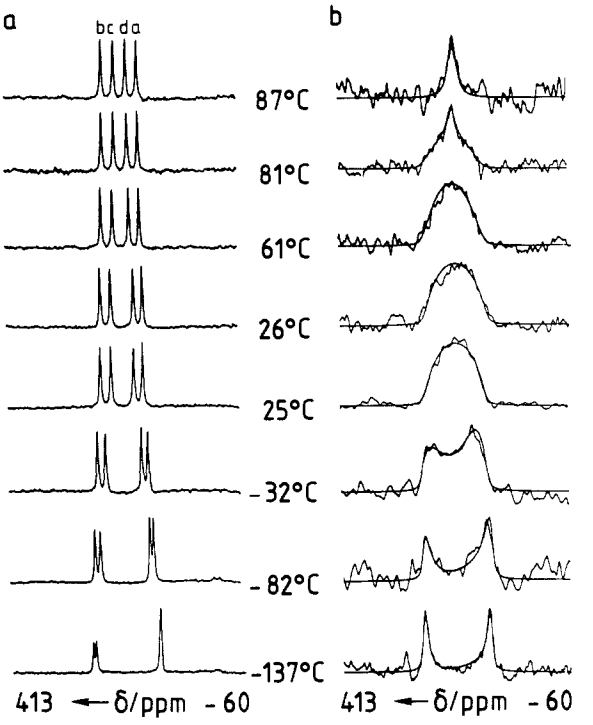


**Figure 6.** $^{15}N$ CPMAS NMR spectra of 95% $^{15}N$ enriched TTAA at 9.12 MHz as a function of temperature: (a) crystalline TTAA; (b) 9.2% TTAA dissolved in polystyrene (from −136 to 25 °C) and 6% TTAA dissolved in polystyrene (from 26 to 87 °C). The spectra were measured with use of a Bruker CXP-100 NMR spectrometer equipped with a Doty[44] probe and a home-built low-temperature heat exchanger[21] and are adapted from ref 24. Experimental conditions: 15 Hz line broadening, 1K/2K zero filling, 6 ms cross polarization time, 10000 Hz sweep width, 2.5 s repetition time, 3 μs $^1H$–$\pi/2$ pulses, quadrature detection, (a) 500 and (b) 20000 scans on average; refrence external $^{15}NH_4Cl$. The spectra in b were calculated as described in the text. Parameters of the calculation: $\nu_{NH} = \nu_{A_2} = \nu_{X_1} = 935$ Hz (102.5 ppm), $\nu_N = \nu_{A_1} = \nu_{X_2} = 2266$ Hz (248.5 ppm); $\Delta = 4.3, 4.0, 2.2, 1.1$ kJ mol$^{-1}$ and $\sigma = 1.5, 2.1, 2.4, 2.6$ kJ mol$^{-1}$ at −137, −82, −32, and 25 °C; $W_0 = 70$ Hz; 20 sites. $\Delta = 1.1, 0.5, 0.5, 0.5$ kJ mol$^{-1}$ and $\sigma = 2.6$ kJ mol$^{-1}$ at 26, 61, 81, and 87 °C; $W_0 = 70$ Hz; 16 sites; $\tau^{-1} = 7000$ and 8000 s$^{-1}$ at 81 and 87 °C; the intensity ratio of the "melted" and the "rigid" signal was 3:7 at 81 °C.

**Crystalline TTAA.** In Figure 6a the $^{15}N$ CPMAS NMR spectra of crystalline TTAA are shown as a function of temperature. In the whole temperature region the spectra of the crystalline material contain four lines of equal intensity, *a–d*, whose frequencies are strongly dependent on temperature. Between −173 and −193 °C, the lowest temperature where experiments were performed, no spectral changes occur,[22] indicating that the intrinsic chemical shifts are temperature independent within the experimental error. Lines *a* and *d* which overlap at low temperatures, were assigned[22] to NH atoms and the two resolved lines *b* and *c* to two inequivalent =N— atoms in solid TTAA. As the temperature is increased, lines *d* and *c* move toward each other without coalescing, as do lines *a* and *b*. The low-field shift of line *a* matches the high-field shift of line *b*. The same is true for lines *d* and *c*. Since the intrinsic chemical shifts are temperature independent these changes can only be explained in terms of fast-exchange processes similar to the situation discussed in Figure 3b, where the line positions were given by eq 18 and 19. These fast processes tend to remove the difference between the NH and the =N— atoms and can, therefore, be identified with fast proton transfers between *a* and *b*, and between *d* and *c*. In other words, as temperature is raised the average proton density on atoms *b* and *c*, respectively, increases at the expense of the average proton density on atoms *a* and *d*, respectively. Thus, we have two proton-transfer systems of the type shown in eq 14, with $AX = ab$ and $dc$, where each system has access to two states $i, j = 1, 2$. Using eq 18–20 the equilibrium constants $K_{12}^{ab}$ and $K_{12}^{dc}$ can be obtained as a function of temperature by analyzing their line positions.[22] Since $K_{12}^{ab} \neq K_{12}^{dc}$

the proton-transfer system *ab* and *dc* are not equivalent. Two-dimensional exchange experiments[22] revealed the existence of spin diffusion between all lines *a* to *d*, arising from dipolar interactions between the nuclei, even if $^{15}N$-labeled material was dissolved in the unlabeled material. This observation was taken as proof that each TTAA molecule contains all four chemically inequivalent nuclei *a* to *d*. Thus, since $K_{12}^{ab} \neq K_{12}^{dc}$ the transfer of the two protons in TTAA must be uncorrelated. Each TTAA molecule can, therefore, exist in four tautomeric states i, j = 1–4, characterized by the equilibrium constants $K_{ij}$, to which the structures shown in Figure 1 have been assigned.[22] These constants are related to those defined above in the following way[22]

$$K_{12}^{ab} = K_{14}(1 + K_{42})/(1 + K_{13}),\ K_{12}^{dc} = K_{13}(1 + K_{32})/(1 + K_{14}) \quad (44)$$

If the two proton-transfer systems *ab* and *dc* are independent of each other, i.e., if

$$K_{14} \approx K_{32} \text{ and } K_{13} \approx K_{42} \quad (45)$$

it follows that

$$K_{12}^{ab} \approx K_{14} \text{ and } K_{12}^{dc} \approx K_{13} \quad (46)$$

When log $K_{12}^{ab}$ and log $K_{12}^{dc}$, measured between −150 and +130 °C, were plotted vs $1/T$ straight lines were obtained from which the reaction enthalpies $\Delta H_{12}^{ab} \approx \Delta H_{14} \approx \Delta E_{14} = 4.5 \pm 0.2$ kJ mol$^{-1}$ and $\Delta H_{12}^{dc} \approx \Delta H_{13} \approx \Delta E_{13} = 4.9 \pm 0.2$ kJ mol$^{-1}$ were obtained. The corresponding reaction entropies almost vanish in view of the finding that $\Delta S_{12}^{ab} \approx \Delta S_{14} = 3.4 \pm 0.5$ J K$^{-1}$ mol$^{-1}$ and $\Delta S_{12}^{dc} \approx \Delta S_{13} = 10 \pm 1$ J K$^{-1}$ mol$^{-1}$.

**TTAA Dissolved in Polystyrene.** We come now to the question of how the tautomerism in a dye such as TTAA is affected when the environment is changed from the crystalline state to a solid solution in a disordered matrix such as glassy polystyrene. The TTAA molecule was ideal for the study of these questions (i) because of its great solubility in glassy polymers and (ii) because complications arising from additional dynamic line broadening due to slow proton transfer as in the case of DTAA[23,32] (Figure 1) are avoided. The experimental and calculated $^{15}N$ CPMAS NMR spectra of TTAA, dissolved at concentrations of 9.2% and 6% p.w. in glassy polystyrene, are shown in Figure 6b. Note the great contrast between these glass spectra and the crystal spectra of Figure 6a. In the room temperature region the glass spectra consist of one broad line that separates into two components as the sample is cooled. These changes could be reproduced very well, although after several temperature cycles the four sharp lines of Figure 6a appeared in the spectra of the 9.2% sample due to slow formation of TTAA microcrystallites. The latter can, thus, be easily distinguished from the dissolved TTAA molecules. Depending on the conditions of sample preparation, an impurity was formed giving rise to the small line at 290 ppm in Figure 6b. Several samples with concentrations between 2% and 10% p.w. were prepared of which spectra were taken at room temperature, but no line shape changes with concentration could be detected in these experiments. In order to establish the nature of the line broadening of the spectra of Figure 6b a two-dimensional exchange experiment[16] on an 8% TTAA/polystyrene sample was performed which revealed a narrow ridge along the diagonal axis as shown in Figure 7. This observation proves that the spectra of TTAA in polystyrene are inhomogeneously broadened, i.e., that they are composed of many sharp lines. If the line broadening were homogeneous, i.e., arising from dynamic processes, the two-dimensional signal would extend in all directions.[16] In view of the poor signal-to-noise ratio no attempt was made to detect possible cross peaks that could arise from spin diffusion.[22]

A comparison of the experimental spectra in Figure 6b with those in Figure 4 shows that the temperature dependent inhomogeneously broadened NMR line shapes can be explained with the presence of a broad distribution of different sites *m* in which the individual $^{15}N$ nuclei experience different equilibrium constants $K_{1m2m}$ of the extremely fast proton tautomerism. The appearance of the characteristic "hole" in the NMR line shapes when the temperature is lowered indicates that the probability of finding

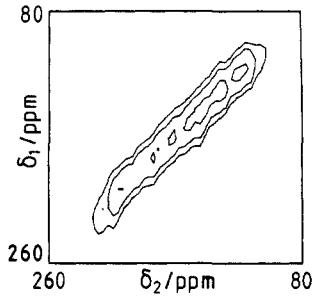


**Figure 7.** Two-dimensional magnetization transfer 9.12-MHz $^{15}N$ CPMAS spectrum (contour plot) at 27 °C of a 8.2% solution of TTAA-$^{15}N_4$ in polystyrene with a mixing time of 1 s. There were 32 by 256 points in the original data matrix, 2048 scans per spectrum. Experimental conditions: 6 ms cross polarization time, 3 μs $^1H$–$\pi/2$ pulses, 2.7 repetition time, reference external $^{15}NH_4Cl$. Reproduced with permission from ref 24. Copyright 1987 VCH.

$^{15}N$ nuclei which experience quilibrium constants of the order of unity decreases. The agreement between the superposed experimental and the calculated spectra in Figure 6b is satisfactory. These calculations with the computer program mentioned in the theoretical section require some further comment. A total of 20 sites were considered weighed according to eq 38. By setting the mean value of the free energy of tautomerism, $\overline{\Delta G_{12}} = 0$, i.e., the mean equilibrium constant of tautomerism $\overline{K_{12}} = 1$, the chemical symmetry of TTAA was taken into account. In the calculations the inverse correlation times $\tau^{-1}$ were set to zero below 65 °C in view of the small individual line widths as indicated by the small ridge in the two-dimensional exchange experiment (Figure 7). By simulation we find individual line widths of the order of $W_0 \approx 70$ Hz, which compares well with the value of $W_0 \approx 50$ Hz for the lines in Figure 6a. $W_0$ is the sum of the residual inhomogeneous line width arising from magic angle misadjustments, magnetic field inhomogeneity artificial line broadening, etc., and the homogeneous line width arising from all possible dynamic processes. The intrinsic chemical shifts of the protonated and the nonprotonated $^{15}N$ atoms were taken to be temperature independent and to be the same in all sites according to eq 24. An intensity correction function $f_m$ (see eq 7) had to be introduced because of the different cross polarization dynamics of the protonated and nonprotonated $^{15}N$ atoms. A linear dependence of $f_m$ on the average proton density was assumed. Since this quantity depends linearly with frequency we used the relation

$$f_m = (\text{constant})m + 1 \quad (47)$$

where the constant was determined by line shape analysis. If possible, the time of the contact pulse was chosen such as to minimize this constant. Additional parameters of the calculations are indicated in Figure 6, the most important being the parameter Δ, characterizing the maximum of the distribution, and the width σ of the distribution, as defined in eq 30–33. We find that Δ, although relatively small, decreases slightly with increasing temperature (see Figure 6b), whereas σ seems to increase.

Since below 65 °C the spectra could be simulated assuming an infinite site lifetime τ, rotational diffusion of TTAA and exchange between different sites must be slow on the NMR time scale in this temperature range. These processes would increase the homogeneous line width and eventually lead to a collapse of the broad lines in Figure 6b into one sharp line as proposed in Figure 5. The top spectra of Figure 6b show what happens when the temperature is increased. In contrast to the predictions of Figure 5, we do not observe a smooth narrowing of the broad line as expected for a monotonous decrease of the site lifetimes τ with temperature. Major line shape changes occur only above 65 °C, where the glass transition region begins according to the DCS data. At the glass transition temperature of about 82 °C the spectrum consists of a relatively sharp center line superimposed on the broad line, indicating that a fraction of the dye molecules has become very mobile, whereas the other fraction is still immobile. As the temperature is further increased the fraction of the mobile dye

molecules increases. At the end of the glass transition region at about 90 °C all dye molecules have become mobile and only the sharp line survives. The NMR line shapes were calculated as a static superposition of two contributions arising from the immobile and the mobile fractions; it was assumed that the parameters describing the width and the maximum of the site distribution are the same for the molecules in the mobile and the immobile phase. Values for the site exchange time of the dyes in the mobile phase were extracted from the spectra as indicated in Figure 6. For the calculations in Figure 6 we arbitrarily used the ASE model where all sites exchange with each other site. A similar result was obtained in terms of the NSE model, although a shorter correlation time had to be used in order to reproduce the experimental line shapes. Thus, we cannot distinguish between the two models at present.

## Discussion

We have described a theory of high-resolution solid-state NMR line shapes of bistable molecules that are subject to rapid exchange between two isomeric forms in the presence of static and dynamic intermolecular interactions which perturb the isomerism. As an example, the solid-state tautomerism of a $^{15}N$-enriched dye, TTAA, has been studied by $^{15}N$ CPMAS NMR spectroscopy in the ordered crystalline state and embedded in a solid solution in glassy polystyrene, below and above the glass transition region.

**Isomerism of Bistable Molecules in an Ordered Rigid Matrix.** First, let us discuss the high-resolution solid-state NMR line shapes of nuclei $A$, $X$ in bistable molecules located in an ordered rigid matrix. Let $K_{12} \leq 1$ be the equilibrium constant of the isomerism $\mathbf{1} \rightleftharpoons \mathbf{2}$. The calculated spectra of $A$ and $X$ are shown in Figure 2a, where four lines $A_1$, $A_2$, $X_1$, and $X_2$ are obtained in the slow and two averaged lines $A$ and $X$ in the fast exchange region. Of practical importance is the case of bistable molecules where the two states **1** and **2** are degenerate in the isolated molecule, rendering the two nuclei $A$ and $X$ chemically equivalent, but where this degeneracy is lifted in the solid state. Consider as an example a dye like TTAA (Figure 1) which contains proton transfer systems of the type $^{15}N_AH\cdots{}^{15}N_X$ (state **1**) $\rightleftarrows$ $^{15}N_A\cdots H^{15}N_X$ (state **2**). Let **1** be favored here over **2** because of solid-state effects. For such molecules the lines $X_1$ and $A_2$ (and also $A_1$ and $X_2$) coincide in the slow exchange regime as shown in Figure 2b. When the exchange becomes faster the lines broaden and coalesce into two averaged sharp lines $A$ and $X$ whose positions depend on $K_{12}$. If $K_{12} \ll 1$ only state **1** is populated (Figure 3b, bottom) and the spectra cannot be distinguished from the slow-exchange case (Figure 2b, bottom). When $K_{12}$ increases line $X$ shifts to low and line $A$ to high field (Figure 3b middle). When $K_{12} = 1$, both lines coincide in the line center (Figure 3, a and b, top).

The pattern of Figure 3b is found in the $^{15}N$ CPMAS NMR spectra of crystalline TTAA[22] as demonstrated in Figure 6a, although four instead of two lines are observed which move toward each other as the temperature is raised. A similar observation was recently made for crystalline porphycen.[20] These spectral changes indicate the presence of two inequivalent $^{15}N_AH\cdots{}^{15}N_X \rightleftarrows {}^{15}N_A\cdots H^{15}N_X$ proton-transfer systems, with $AX \equiv ab$ and $dc$ (Figure 1) in crystalline TTAA, characterized by different equilibrium constants of tautomerism.[22] Thus, crystalline TTAA contains four inequivalent $^{15}N$ atoms with different average proton densities. Two-dimensional NMR exchange experiments indicated spin diffusion between all four lines.[22] From this observation it was concluded that each TTAA molecule contains both types of proton-transfer systems. Therefore, each TTAA molecule exists in all four possible tautomeric states proposed in Figure 1 which interconvert rapidly with respect to the time scale provided by the $^{15}N$ chemical shifts. The temperature-dependent proton densities arise from the fact that the equilibrium constants of tautomerism are temperature dependent. From these observations it follows that the gas-phase degeneracies between the "diagonal" tautomers **1** and **2** and the vicinal tautomers **3** and **4** are lifted in the crystal by intermolecular interactions. Note that these results indicate that TTAA cannot rotate in the crystal, neither around the axis perpendicular to the molecular plane nor around axes that are located in this plane. Such rotations would result in an exchange of the different nitrogen atoms and lead to equal average proton densities $^1/_2$ on all $^{15}N$ atoms $a$ to $d$, and all lines $a$ to $d$ in Figure 6a would broaden and coalesce into a single sharp line. However, even at 87 °C we were not able to detect such line broadening due to rotations.

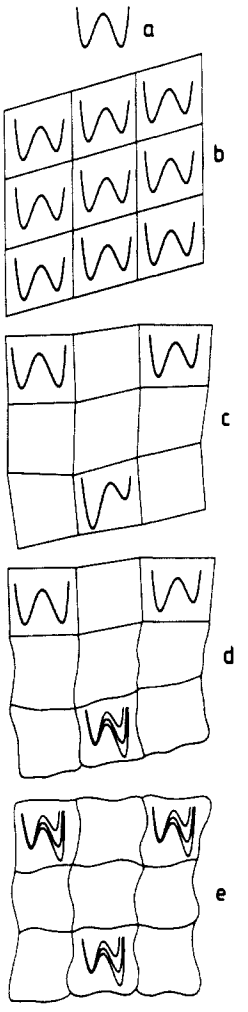


**Figure 8.** Perturbation of a double minimum potential of a bistable molecule by intermolecular interactions: (a) symmetric double minimum potential in the gas phase; (b) perturbation of the potential in the ordered solid state by intermolecular interactions leading to one molecular site; (c) perturbation of the potential in the disordered solid state by intermolecular interactions leading to a distribution of different sites; (d) motional averaging within the NMR time scale of the potentials in the melted regions of the disordered solid state by molecular motions in the region of the glass transition (partial site exchange); (e) complete motional averaging of all sites above the glass transition.

A similar perturbation of the tautomerism was recently found for crystalline DTAA (Figure 1), although only the two "diagonal" tautomers **1** and **2** in Figure 1 were found.[23] In addition, in contrast to TTAA, experimental spectra of the type shown in Figure 2b indicated that the two states interconverted slowly on the NMR time scale. Such solid-state effects on bistable molecules can be modeled as illustrated schematically in Figure 8, a and b. Consider for simplicity, but without loss of generality, a double minimum potential that is symmetric in the gas phase (Figure 8a). The reaction entropy $\Delta S_{12}$ and the reaction energy $\Delta E_{12}$ between the two states vanish. In the bulk crystal or in a crystalline host the gas-phase degeneracy will be lifted if the reacting molecules are placed in a nonsymmetric way with respect to an existing preferential axis (Figure 8b). In a first approximation, the double minimum potential of one molecule will be independent of the molecular state of the neighboring molecules. In addition, $\Delta S_{12}$ is still close to zero. In an ordered environment such as a crystal lattice, all molecules will then be characterized by the same

energy difference $\Delta E_{12} \neq 0$ between the two wells of the double minimum potential. For TTAA and DTAA we find $\Delta E_{12}$ values of the order of 4 kJ mol$^{-1}$. It depends in a sensitive way on the interplay between the molecular structure and the intermolecular interactions. We also find that $\Delta S_{12} \approx 0$.

For the case that the potential curve of a given molecule would depend on the molecular state of the surrounding molecules one would expect an order–disorder transition at higher temperatures.

**Isomerism of Bistable Molecules in a Disordered Rigid Matrix.** From optical studies[7-11] it is known that molecules embedded in disordered rigid matrices can experience a broad distribution of different environments or "sites". In view of the above results it is then understandable that bistable molecules, which can exist in two stable isomeric forms **1** and **2**, should experience in the different sites different equilibrium constants $K_{12}$ of the isomerism. As shown in this study such distributions of equilibrium constants can be monitored by NMR if each site contains only one type of spin and if the exchange between the isomeric forms is fast on the NMR time scale. Then each site contributes only one averaged line to the NMR spectrum with a line position given by $K_{12}$ and a line intensity given by the number of bistable molecules in this site. Calculated spectra are shown in Figure 4, where a small number of sites has arbitrarily been chosen in order to demonstrate that the spectra are the static sum of superposed sharp lines. For a larger number of sites all individual lines overlap, giving rise to one "inhomogeneously" broadened line. In the calculations of the spectra in Figure 4 the sites are weighed using a bigaussian distribution of the free reaction enthalpy $\Delta G_{12} = -RT \ln K_{12}$ values of the isomerism (eq 32), characterized by the maxima $\overline{\Delta G_{12}} \pm \Delta$ and the width $\sigma$. $\overline{\Delta G_{12}}$ is the mean free reaction enthalpy. The different spectra of Figure 4 correspond to different values of $\Delta$ and $\sigma$. In Figure 4 $\overline{\Delta G_{12}}$ was set to zero, which signifies that the mean value $\bar{K}_{12} = 1$. This case is typical for reaction systems with double minimum potentials that are symmetric in the gas phase. It is clear that for such reaction systems (like TTAA) positive and negative perturbations must have the same probability, as assumed in Figure 4. In other words, the probability of finding a site with an equilibrium constant $K_{12}$ is equal to the probability of finding the "twinned" site with the inverse equilibrium constant $K_{12}^{-1}$. Therefore, the line shape is symmetric about the line center. Thus it becomes clear that the function characterizing the distribution of equilibrium constants can be directly obtained from the NMR spectra. Note that in the case of $^{15}N$ NMR of NH···N proton transfer systems this distribution function is equivalent to the function describing the probability $P(x)$ of finding a $^{15}N$ atom with a given proton density $x$.

As a comparison of Figures 4 and 6b shows, the experimental $^{15}N$ CPMAS NMR spectra of TTAA embedded in glassy polystyrene can very well be simulated below the glass transition by using the above theory of inhomogeneous NMR line broadening. The contrast between these glass spectra and the corresponding crystal spectra (Figure 6a) is striking. At first sight the glass spectra could be confounded with the case of Figure 3a where slow isomerism leads to dynamic line broadening. However, two-dimensional NMR experiments according to Figure 7 show that the broad lines of TTAA in glassy polystyrene are inhomogeneously broadened. In view of the rather limited signal-to-noise ratio it can, however, not be excluded that, besides the bigaussian distribution function used here, there might also be other functions that can accommodate the experimental data. Finally, it is interesting to note that, as in the case of crystalline TTAA, we can exclude also for the glassy TTAA solution below the glass transition temperature that the dye rotates fast in the glass. Again, such rotations would lead to dynamic line broadening and coalescence of all the components of the inhomogeneous broadened lines in Figure 6b.

These results lead to a molecular model, shown in Figure 8c, of how a symmetric double minimum potential of an isolated bistable molecule in the gas phase (Figure 8a) is perturbed by intermolecular interactions when the molecule is embedded in disordered condensed media such as a glass. In this environment the periodicity of the unit cells in which the bistable molecule is located has been lost, as is indicated schematically in Figure 8c. The double minimum potential is distorted in a different way depending on the environment, leading to a continuous distribution of $\Delta G_{12}$ values of the isomerism. The model represents a snapshot of reacting molecules in disordered condensed matter, in a time scale of slow molecular motion, i.e., it might be applied not only to glasses but also to liquids, however, in a much shorter time scale, as realized, for example, in IR spectroscopy. Thus, results of both NMR and IR experiments on glassy solutions may be directly compared because both methods see the observed molecules as immobile.

It is interesting to note that the free reaction energies characterizing the tautomerism of TTAA in the crystal compare well with the most probable free reaction energy $\Delta$, defined in eq 32, for the glassy solution in polystyrene. $\Delta G_{12}^{ab}$ and $\Delta G_{12}^{dc}$ decrease from 4 and 3.3 kJ mol$^{-1}$ at −137 °C to 3.3 and 1.3 kJ mol$^{-1}$ at +87 °C. In this range $\Delta$ changes from 4.3 to 1.1 kJ mol$^{-1}$. At the same time the width $\sigma$ of the distribution increases from 1.5 to 2.6 kJ mol$^{-1}$. At present the margin of error of $\Delta$ and $\sigma$ is too large in order to know whether these results indicate temperature-independent $\Delta H_{12}$ and $\Delta S_{12}$ values of the individual sites or whether these values are temperature dependent due to structural changes of the matrix.

Note that, in principle, the molecules in a given site have further to be divided into "subsites" characterized by different rate constants of exchange between the molecular states **1** and **2**. In this study it was not necessary to introduce such subsites because we deliberately restricted ourselves to the case of fast state exchange. We reserve this more complicated case of the presence of a distribution of equilibrium constants *and* rate constants for a future study.

**Isomerism of Bistable Molecules in a Mobile Matrix.** The last question we have to address is how exchange between the different sites affects the NMR spectra and how this exchange occurs in reality. The calculated spectra depend on the details of the site-exchange process. The results of two different site-exchange models that employ only a single correlation time $\tau$ are shown in Figure 5. Both models predict in the fast site exchange regime a liquid-type NMR spectrum characterized by a motionally averaged equilibrium constant $\bar{K}_{12} = \exp(-\overline{\Delta G_{12}}/RT)$ of the isomerism. Since for the symmetric N–H···N proton transfer compound studied here $\overline{\Delta G_{12}} = 0$, i.e., $\bar{K}_{12} = 1$, only one sharp $^{15}N$ line arises in the fast site exchange regime at the signal center because all nitrogen atoms experience then the same average proton density $^1/_2$ within the NMR time scale. Note that in the case of symmetric bistable molecules like TTAA exchange between different sites, i.e., $^{15}N$ atoms with different average proton densities, can occur via rotations as mentioned above or via motions of the surrounding molecules. Both processes are probably strongly coupled. Since only one single site correlation time is employed in the models leading to the spectra in Figure 5 it is not possible to decide the type of molecular motion leading to the apparent symmetric double minimum potentials of the proton motion in the fast site exchange regime. Note, however, that in the neighbor site model (NSE) where the equilibrium constants $K_{12}$ change only in small increments, rotations are practically excluded. By contrast, they are taken into account in the all site model (ASE) in view of the fact that a 180° rotation of the molecule changes the equilibrium constant from the value $K_{12}$ to its inverse $K_{12}^{-1}$.

As expected from Figure 5, a sharp center line was observed experimentally in the $^{15}N$ CPMAS NMR spectra of TTAA in polystyrene in the temperature region of the glass transition where the molecular motion of the matrix molecules becomes fast (Figure 6b, top). However, we did not find a smooth decrease of the correlation time $\tau$ of the site exchange but a static superposition of "rigid" sites with $\tau \gg (\pi\Delta\nu)^{-1}$, where $\Delta\nu$ is the chemical shift difference between NH and N nuclei, and of "melted" sites with short site lifetimes $\tau \ll (\pi\Delta\nu)^{-1}$. Sites with $\tau \approx (\pi\Delta\nu)^{-1}$ might be present in a low, nonobservable concentration, which is understandable if there is a very broad distribution of site-exchange

correlation times. Similar separation in two phases, one characterized by long and the other by short correlation times of molecular motions, has been found previously by NMR for organic glasses.[17,51,52]

The situation is depicted schematically in Figure 8d. In the rigid sites the dye molecules are more or less stuck and still characterized by an asymmetric double minimum potential of proton tautomerism, whereas in the melted regions they experience a motionally averaged symmetric double minimum potential. The latter is fundamentally different from the symmetric gas-phase potential of Figure 8a because the potential is *never* really symmetric but only on average. As shown in Figure 8e, all sites experience the same motionally averaged double minimum potential above the glass transition and can, therefore, no longer be distinguished by $^{15}N$ NMR. The extension of this model to asymmetric gas-phase double minimum potentials is straightforward. Note that the glass transition was monitored by NMR at exactly the same temperature $T_g$ as by DSC. The residual solvent and the dye molecules apparently act as additives, which are known to reduce $T_g$ with respect to pure polystyrene.[51]

## Conclusions

We conclude that information on fast chemical reactions under conditions of slow solvent reorientation can be obtained by solid solution state NMR. When analyzing exchange broadened NMR spectra of bistable molecules, subject to a molecular isomerism, in the disordered solid state, inhomogeneous line broadening arising from a distribution of equilibrium constants of the isomerism has to be taken into account. We propose to use the width of the corresponding distribution function which is directly accessible by NMR as a qualitative measure of local order experienced by dyes or other additives in glasses, the crystalline state serving as a reference for perfect ordering. In addition, dyes like TTAA can also be used to indirectly monitor the motion of the surrounding molecules, which leads to a motional averaging of the double minimum potentials of the two-state exchange via exchange between the different sites. The fine details of the latter have still to be elucidated. Finally, kinetic theories of chemical reactions in condensed disordered matter have to take into account distributions of double minimum potentials with different transition state and reactant energies arising from intermolecular interactions.

**Acknowledgment.** We thank Dr. C. S. Yannoni and R. D. Kendrick, IBM Almaden Research Laboratory, San Jose, for their contributions to this work. The DSC measurements were kindly performed by G. Kögler, Institut für Makromolekulare Chemie der Universität Freiburg. We also thank the Deutsche Forschungsgemeinschaft, Bonn-Bad Godesberg, the Stiftung Volkswagenwerk, Hannover, and the Fonds der Chemischen Industrie, Frankfurt, for financial support.

**Registry No.** TTAA, 116128-66-6; NiTTAA, 116651-11-0; PS, 9003-53-6; OPDA, 116006-97-4; $^{15}NH_3$, 13767-16-3; *o*-dichlorobenzene, 95-50-1; acetylacetone, 123-54-6.

(51) Spiess, H. W. *Coll. Pol. Sci.* **1983**, *261*, 193. Wehrle, M.; Hellmann, G. P.; Spiess, H. W. *Ibid.* **1987**, *265*, 815.
(52) English, A. D.; Zoller, P. *Anal. Chim. Acta* **1986**, *189*, 135.

# $^{59}Co$ NMR of Cobalt(III) Porphyrin Complexes. 2. Electric Field Gradients, d-Orbital Populations, and Hydrogen Bonding

**Karen I. Hagen, Catherine M. Schwab, John O. Edwards,* John G. Jones,[1] Ronald G. Lawler, and Dwight A. Sweigart[2]**

*Contribution from the Department of Chemistry, Brown University, Providence, Rhode Island 02912.* *Received November 27, 1987*

**Abstract:** A series of six-coordinate cobalt(III) tetraphenylporphyrin complexes with para substituents on the phenyl groups and with a variety of axial imidazole ligands has been prepared. The $^{59}Co$ NMR spectra of these complexes in a number of solvents and at several field strengths are reported. Shielding anisotropy is very small, confirming our earlier suggestion that porphyrin, imidazole, and ammonia ligands have nearly the same position in the spectrochemical series. The chemical shift $\delta$ and line width $\omega_{1/2}$ increase as the para substituent on the TPP phenyl rings becomes electron-releasing. Correlations of $\delta$ and $\omega_{1/2}$ with Hammett $\sigma$ substituent constants are noted. A simple molecular orbital model is used to rationalize both chemical shift and line width changes. It is concluded that variations in $\omega_{1/2}$ with substitutent arise from changes in the electric field gradient, $q$, which in turn depends on the extent of mixing of metal 3d and ligand $\pi$ orbitals. The chemical shift and line width also depend on the substituent on the imidazole N-1 nitrogen. In particular, hydrogen bonding to solvent or added base from axial imidazoles containing the N–H group strongly affects $\omega_{1/2}$, and the conclusion is reached that $^{59}Co$ NMR is a good way to study such "proximal" hydrogen-bonding interactions. The $^{59}Co$ NMR spectra are dominated by quadrupolar relaxation, and this is discussed along with other possible relaxation mechanisms.

$^{59}Co$ NMR is relatively easy to perform and is a useful technique to probe the electronic interactions in cobalt(III) porphyrins. This, in turn, provides information that should be applicable to iron porphyrins since Co(III) has the same charge and nearly the same size as Fe(III) and is isoelectronic with low-spin Fe(II). Substituting cobalt for iron in NMR studies is particularly attractive in view of the great difficulty in obtaining $^{57}Fe$ NMR. In a recent article we reported[3] the $^{59}Co$ NMR of $Co(Por)(RIm)_2^+$ complexes, where Por is the dianion of tetraphenylporphyrin (TPP) or octaethylporphyrin (OEP) and RIm is imidazole (R = H) or *N*-methylimidazole (R = Me). This work suggested that (1) ammonia, imidazole, and porphyrin ligands are very close in the spectrochemical series, (2) hydrogen bonding from the N–H hydrogen of coordinated imidazole significantly affects the chemical shift and line width, (3) substituent changes at the

(1) Permanent address: Department of Chemistry, University of Ulster, Coleraine, Northern Ireland, BT52 1SA.
(2) Recipient NIH Research Career Development Award, 1983-1988.
(3) Hagen, K. I.; Schwab, C. M.; Edwards, J. O.; Sweigart, D. A. *Inorg. Chem.* **1986**, *25*, 978.

0002-7863/88/1510-7024$01.50/0 